INTERNATIONAL JOURNAL OF ENVIRONMENT, ENGINEERING & EDUCATION

ISSN 2656-8039 (ONLINE)
VOLUME 8 • ISSUE 1 • MARCH 2026

Received: 18 June 2025 | Accepted: 20 January 2026 | Published: 1 March 2026

Research Article

# Predictive Modeling of NaOCl Dosage for Iron Removal in a Combined Aeration–Oxidation System Using Gene Expression Programming

Ruba Dahham Alsaeed [a,*] • Heba Aljaddou [a] • Diala Shehab [b] • Bassam Alaji [c] • Durgam Salloum [d]

[a] Faculty of Civil Engineering, Al-Wataniya Private University, Hama, Syria | [b] Faculty of Civil Engineering, Wadi International University, Homs, Syria
[c] Department of Environmental Engineering, Damascus University, Damascus, Syria | [d] Faculty of Civil Engineering, Homs University, Homs, Syria

## ABSTRACT

Iron is one of the most prevalent groundwater contaminants and can cause significant aesthetic, operational, and infrastructural problems when present at elevated concentrations. This study aims to (i) experimentally evaluate the effects of pH, dissolved oxygen (DO), and sodium hypochlorite (NaOCl) dosage on iron removal efficiency, and (ii) develop an interpretable Gene Expression Programming (GEP) model to predict the optimal NaOCl dose under varying water-quality conditions. Laboratory jar test experiments demonstrated that iron oxidation is strongly pH-dependent, with maximum removal efficiency (up to 99%) achieved under acidic conditions (pH 4) at a NaOCl dose of 6 mg/L, due to the predominance of hypochlorous acid. Under practical near-neutral conditions relevant to drinking-water treatment (pH 6.5–7.5), aeration alone enhanced iron removal as DO increased, although diminishing returns were observed beyond 6 mg/L DO due to increased energy demand. A combined treatment strategy involving low-dose pre-chlorination followed by aeration exhibited a clear synergistic effect, achieving iron removal efficiencies of approximately 85–89% using NaOCl doses of 1–3 mg/L and DO levels of 4–5 mg/L. This approach reduced overall operational costs by approximately 40% compared with aeration-only treatment. The developed GEP model showed strong predictive performance ($R^2$ = 0.94; RMSE = 0.34 mg/L) and generated explicit mathematical expressions linking oxidant demand to pH, DO, and influent iron concentration. Overall, the study confirms the technical and economic advantages of pre-chlorination combined with aeration and highlights the potential of GEP as a transparent decision-support tool for optimizing groundwater iron removal.

**KEYWORDS** contaminated • cost–performance optimization • dissolved oxygen control • groundwater treatment • oxidation kinetics • water ecosystems

**ARTICLE CITATION**
R. D. Alsaeed, H. Aljaddou, D. Shehab, B. Alaji, D. Salloum "Predictive Modeling of NaOCl Dosage for Iron Removal in a Combined Aeration–Oxidation System Using Gene Expression Programming," International Journal of Environment, Engineering and Education, Vol. 8, No. 1, pp. 1-18, 2026.
https://doi.org/10.55151/ijeedu.v8i1.235

***CORRESPONDENCE**
Ruba Dahham Alsaeed ruba.alsaeed@wpu.edu.sy Faculty of Civil Engineering, Al-Wataniya Private University, Hama Governorate - International Highway (Hama-Homs), Hama, Syria. https://orcid.org/0000-0002-4848-5348

## 1. INTRODUCTION

Groundwater is a vital source of water for drinking, agriculture, and industrial activities, particularly in arid and semi-arid regions where surface water resources are scarce or unreliable. Its widespread use is largely attributed to its perceived microbiological safety, resulting from natural filtration through geological formations, as well as its broad availability and relative resilience to seasonal variability, climate change impacts, and accidental contamination events [1], [2]. Consequently, many rural communities and small- to medium-sized municipalities rely predominantly, and in some cases exclusively, on groundwater supplies that typically require limited treatment. This reliance underscores the critical role of groundwater in ensuring water security and continuity of supply in vulnerable regions.

Despite its generally high microbial quality, groundwater frequently contains elevated concentrations of dissolved minerals, particularly iron. Although iron is not considered toxic at typical concentrations, excessive levels pose significant aesthetic, operational, and infrastructural challenges when they exceed recommended limits [3]. The World Health Organization (WHO) recommends a guideline value of 0.3 mg/L for iron in drinking water to prevent undesirable taste, discoloration, staining of fixtures and laundry, and clogging of water distribution systems [4]. However, iron concentrations in groundwater can vary widely and may exceed 50 mg/L, especially in anaerobic aquifers where dissolved ferrous iron ($Fe^{2+}$) predominates [5].

Iron is one of the most abundant elements in the Earth's crust and is commonly mobilized into groundwater through the dissolution of iron-bearing minerals such as oxides, sulfides, carbonates, and silicates under reducing conditions. In such environments, iron exists primarily in its soluble ferrous form ($Fe^{2+}$), which remains stable in the absence of oxygen [5]. Upon abstraction and exposure to oxidizing conditions, $Fe^{2+}$ is rapidly converted to ferric iron ($Fe^{3+}$), leading to the formation and precipitation of insoluble iron hydroxides and oxyhydroxide phases, such as $Fe(OH)_3$ [6]. These precipitates are responsible for reddish-brown discoloration, metallic taste, and staining of plumbing fixtures and sanitary ware, significantly reducing consumer confidence in the supplied water.

From an operational perspective, iron precipitation in treatment facilities and distribution networks can lead to pipe clogging, increased hydraulic resistance, biofouling, and accelerated corrosion. These processes increase maintenance requirements, reduce hydraulic capacity, and shorten the lifespan of infrastructure. Furthermore, iron deposits can promote the growth of iron-related bacteria, exacerbating water quality degradation and operational instability. Consequently, iron removal is not merely a regulatory obligation but a fundamental technical requirement in groundwater-based drinking water systems. Effective de-ironing is essential to maintaining distribution system performance, ensuring operational reliability, protecting infrastructure from fouling and corrosion, preserving aesthetic water quality, and ultimately sustaining public acceptance of groundwater-derived drinking water supplies. These considerations are central to the long-term sustainability and social viability of groundwater use.

In many groundwater sources, ferrous iron co-occurs with other reduced species such as manganese ($Mn^{2+}$), ammonium ($NH_4^+$), hydrogen sulfide ($H_2S$), and occasionally arsenic in its trivalent form (As (III)). The presence of these co-contaminants strongly influences process selection, treatment sequencing, and overall system design. As a result, a wide range of iron removal technologies has been developed and implemented. The most widely applied ex situ approach is oxidation–filtration, in which oxidants such as dissolved oxygen or chlorine are used to oxidize $Fe^{2+}$ to $Fe^{3+}$, followed by filtration of the resulting precipitates [7]. The efficiency of this process is highly dependent on water chemistry, particularly pH, dissolved oxygen concentration, and iron speciation [8].

Alternative treatment methods have been developed to address specific operational conditions. Ion exchange is typically applied at low iron concentrations and in systems requiring simultaneous hardness removal, while chemical precipitation is more suitable for iron concentrations exceeding 10 mg/L [9]. Biological iron removal has gained increasing attention as a sustainable, chemical-free alternative [10], whereas polyphosphate dosing is sometimes used to sequester iron and prevent staining without removing it [11]. Membrane-based processes, such as ultrafiltration, can also be employed to remove iron precipitates following oxidation physically [12]. In addition to surface-based treatments, in situ techniques—most notably the Vyredox process—aim to remove iron within the aquifer itself by establishing an oxygenated reactive zone around abstraction wells, promoting heterogeneous adsorption and localized oxidation of $Fe^{2+}$ on aquifer grains [13], [14]. Such approaches are particularly attractive where surface treatment capacity is limited.

Despite the proven effectiveness of aeration and chemical oxidation technologies, several critical challenges persist. Chief among these is the optimization of oxidant dosing, particularly when chlorine-based oxidants are employed, due to the associated risk of disinfection by-product (DBP) formation and its implications for public health. Treatment sequencing—specifically the comparative performance of pre-chlorination versus post-aeration chlorination—has received limited systematic attention in the existing literature. Moreover, recent studies have highlighted the lack of dynamic, data-driven models capable of predicting the minimum oxidant dose required to achieve a specified effluent iron concentration under varying influent conditions, including pH, dissolved oxygen, and initial iron

levels. Explicit techno-economic analyses that jointly consider chemical consumption and aeration energy requirements are also notably scarce.

Accordingly, three key knowledge gaps can be identified: (i) limited quantitative evidence comparing the effectiveness of pre-chlorination followed by aeration versus the reverse treatment sequence under equivalent operating conditions; (ii) the lack of operationally interpretable models for estimating optimal oxidant dosages across a wide range of groundwater chemistries; and (iii) insufficient reporting of cost trade-offs that integrate both chemical inputs and aeration energy consumption. To address these gaps, the present study investigates the combined application of aeration and chemical oxidation using sodium hypochlorite (NaOCl) for iron removal from groundwater. While the individual processes are well established, their quantitative synergy—particularly the potential kinetic advantage of pre-chlorination in reducing downstream aeration energy demand—has not been rigorously examined using data-driven modeling approaches. This study contributes to the literature by systematically evaluating treatment sequencing and developing a transparent Gene Expression Programming (GEP) model to predict optimal oxidant dosages, thereby supporting cost-effective, evidence-based decision-making for groundwater treatment utilities.

## 2. LITERATURE REVIEW

### 2.1. Chemical Oxidation and Aeration Kinetics for Iron Removal

Iron removal from groundwater has traditionally relied on oxidation-based treatment processes, in which soluble ferrous iron ($Fe^{2+}$) is oxidized to insoluble ferric iron ($Fe^{3}$), followed by solid–liquid separation via sedimentation or filtration. Early foundational studies established the baseline effectiveness of aeration for iron oxidation [15]. They demonstrated the influence of oxidant type, dosage, and pH on the simultaneous removal of iron and manganese using chlorine-based oxidants, including sodium hypochlorite (NaOCl) [16], [17]. Owing to its simplicity and the absence of chemical addition, aeration remains one of the most widely applied iron removal techniques. However, its performance is highly sensitive to operational parameters, including pH, temperature, oxygen transfer efficiency, and hydraulic retention time.

In practice, achieving regulatory iron limits solely through aeration often requires high energy inputs, extended contact times, or large reactor volumes. These requirements can substantially increase operational costs and limit the feasibility of aeration-based systems, particularly for small-scale or decentralized water supply schemes. Chemical oxidation using chlorine-based oxidants offers faster reaction kinetics and improved robustness at moderate iron concentrations. Kan et al. reported that NaOCl oxidation combined with membrane filtration achieved manganese removal efficiencies exceeding 90% at pH values above 7 and oxidant doses greater than 3 mg/L, with the accumulation of iron–manganese oxides enhancing long-term treatment performance [18]. Similarly, Faye et al. investigated iron oxidation kinetics using oxygen, potassium permanganate, and NaOCl, concluding that aeration or chlorination alone was often insufficient to consistently meet drinking water standards under variable groundwater conditions [19]. These findings underscore the strong dependence of chemical oxidation performance on water chemistry and process control.

More recent studies have shown that iron removal is governed not only by homogeneous oxidation and floc formation in solution but also by adsorption onto filter media or preformed flocs, followed by surface-mediated oxidation processes [20]–[22]. While these insights have improved mechanistic understanding, many published studies still report oxidant performance empirically, without providing quantitative guidance on dose optimization or sufficiently elucidating the roles of pH and dissolved oxygen under dynamic operating conditions.

### 2.2. Combined and Alternative Iron Removal Technologies

To address the limitations of single-process systems, combined treatment schemes integrating aeration and chemical oxidation have been increasingly implemented in groundwater treatment practice. These hybrid configurations can enhance removal efficiency and operational resilience; however, their effectiveness is strongly influenced by system design and treatment sequence. Despite the widespread application of aeration–chlorination systems, most studies focus on overall removal performance and compliance outcomes, rather than systematically evaluating the impact of treatment order—such as pre-chlorination followed by aeration versus aeration followed by chlorination. Consequently, treatment design and operational strategies are often based on empirical assumptions, introducing uncertainty in chemical dosing requirements and energy consumption.

In parallel, alternative iron removal technologies have been investigated. Catalytic filtration using $MnO_2$-coated or naturally catalytic media has demonstrated high iron and manganese removal efficiencies at relatively low influent concentrations (<10 mg $L^{-1}$), with performance strongly influenced by media mineralogy and pH [23]. Biological iron-removal processes that exploit iron-oxidizing bacteria to facilitate oxidation without chemical oxidants have also shown promising results under stable operating conditions. Nevertheless, both catalytic and biological approaches are associated with operational challenges, including sensitivity to fluctuations in water chemistry, extended start-up periods, process instability, and increased maintenance demands.

These constraints limit their broader applicability, particularly in resource-constrained or decentralized water supply contexts.

Recent critical reviews confirm that iron and manganese removal from groundwater remains an active and evolving research field, with growing emphasis on advanced and engineered filter media. A comprehensive review highlights recent developments in filter material design, surface modification strategies, and multifunctional treatment pathways that integrate oxidation, adsorption, and catalytic mechanisms [24]. These studies emphasize that media surface properties, material composition, and site-specific operational conditions play decisive roles in treatment robustness and long-term performance, especially during the transition from laboratory-scale experiments to full-scale implementation.

Despite these advances, persistent challenges remain, including site-specific variability, sensitivity to influent water chemistry, and the lack of systematic evaluation frameworks to support process optimization. This reinforces the need for integrated approaches that combine experimental investigation with data-driven, interpretable modeling tools, as pursued in the present study.

### 2.3. Data-Driven Modeling in Drinking Water Treatment

In recent years, data-driven modeling techniques have been increasingly applied in drinking water treatment to predict process performance and optimize chemical dosing strategies [25]. Machine learning approaches such as artificial neural networks (ANNs), support vector machines (SVMs), and gene expression programming (GEP) have demonstrated strong potential for modeling the complex, non-linear relationships inherent in water treatment processes. Among these methods, GEP offers distinct advantages due to its ability to generate explicit mathematical expressions and its high degree of interpretability, enabling practitioners to understand the influence of individual input variables on model outputs.

Previous studies have successfully applied GEP to a range of water treatment applications, including the optimization of poly-aluminum chloride (PACl) dosage [26], modeling manganese and ammonium removal [27], alum dosing strategies [28], turbidity prediction [29], and dissolved organic carbon (DOC) removal [30], [31]. By developing predictive models, it becomes possible to identify the minimum effective chemical dose required to achieve treatment objectives under varying influent conditions, thereby enhancing treatment efficiency while reducing chemical consumption and the risk of disinfection by-product (DBP) formation. However, despite these advances, dynamic and data-driven predictive models specifically targeting oxidant dosage optimization for iron removal remain notably scarce in the literature.

### 2.4. Gene Expression Programming for Dose Prediction and Process Control

Gene Expression Programming (GEP) has emerged as a powerful tool for predicting optimal chemical dosing and supporting process control in water treatment systems. Compared to traditional machine learning techniques such as ANNs and SVMs, GEP offers superior transparency and interpretability, as it produces closed-form mathematical expressions that explicitly describe the relationship between input variables and process outcomes.

#### 2.4.1. Interpretability

A key strength of GEP lies in its ability to generate explicit algebraic equations that engineers and operators can readily interpret. Unlike ANN and SVM models, which often function as “black boxes,” GEP-based models provide actionable insights into process behavior and variable interactions. This interpretability is particularly valuable in operational settings where regulatory compliance, process transparency, and informed decision-making are essential [32]–[34].

#### 2.4.2. Closed-Form Expressions:

Another important advantage of GEP is its ability to produce closed-form solutions that directly relate input parameters—such as pH, dissolved oxygen, temperature, and chemical concentrations—to outputs such as iron removal efficiency or optimal oxidant dosage. In contrast, ANN and SVM models typically rely on iterative numerical procedures and lack explicit analytical expressions, limiting their applicability for real-time process control and optimization [35], [36].

#### 2.4.3. Comparison with ANN and SVM

Although ANNs and SVMs are well-established tools in water treatment modeling, they have limitations in interpretability, computational intensity, and practical implementation. ANNs involve complex neuron architectures, while SVMs rely on kernel transformations that are difficult to interpret without specialized expertise. These models often require extensive training and iterative computation to generate predictions, which can constrain their use in operational environments [37]–[39].

### 2.5. Disinfection By-Products and the Need for Data-Driven Optimization

A major limitation of chlorine-based oxidation processes is the potential formation of harmful disinfection by-products (DBPs) resulting from reactions between chlorine and natural organic matter. Optimizing oxidant dosage is therefore critical, as interactions among chlorine, humic substances, and particulate or colloidal iron can significantly increase regulated DBP formation, intensifying the trade-off between effective iron removal and public health protection [5]. Overdosing increases

DBP risk and unnecessary chemical use, while underdosing may lead to incomplete iron oxidation and unstable treatment performance.

Despite growing interest in advanced process control strategies, the literature reveals a clear lack of dynamic, data-driven models capable of predicting optimal oxidant dosages under variable operational conditions. Although artificial intelligence and machine learning methods are increasingly applied in water treatment research, their use in iron removal optimization particularly for combined aeration–oxidation systems with explicit consideration of DBP minimization remains limited. Furthermore, explicit techno-economic analyses comparing alternative treatment sequences and strategies are rarely integrated into performance evaluations, restricting the practical applicability of existing findings.

Accordingly, the present study addresses these gaps by systematically evaluating the combined use of aeration and sodium hypochlorite oxidation for groundwater iron removal, with particular emphasis on treatment sequencing, oxidant dose optimization, and cost-effectiveness. By integrating experimental analysis with Gene Expression Programming–based modeling, this study aims to provide a transparent and operationally relevant framework for optimizing iron removal while minimizing DBP formation and overall treatment costs.

## 3. MATERIALS AND METHODS

### 3.1. Water Sample Source

Water samples were collected from the Al-Mashrafah groundwater well, located in the Al-Mashrafah district, approximately 20 km from the center of Homs City, Syria. The well supplies potable water to the local village and has a total depth of 386.75 m. In this study, the first set of experiments focused on chemical oxidation using sodium hypochlorite, followed by sedimentation and filtration. The physicochemical characteristics of the water samples across the four experimental series are summarized in Table 1.

Samples were collected in pre-cleaned high-density polyethylene (HDPE) bottles, transported on ice, and analyzed within 6 h of collection. The pH of the samples was adjusted using 0.1 M $H_2SO_4$ or 0.1 M NaOH and verified with a calibrated pH probe (accuracy ±0.01). Jar test experiments were conducted in accordance with ASTM D2035, consisting of rapid mixing at 150 rpm for 2 min, slow mixing at 20 rpm for 15 min, and a settling period of 90 min unless otherwise specified. After settling, the supernatant was filtered through a 0.45-µm membrane filter before analysis.

**Table 1.** Experimental dataset summary (n = 56)

| Parameter | Unit | Mean | SD | Parameter |
|---|---|---|---|---|
| pH | – | 7.5 | 1.46 | pH |
| Iron (Fe) | mg $L^{-1}$ | 1.5 | 0.28 | Iron (Fe) |
| Dissolved Oxygen (DO) | mg $L^{-1}$ | 4.0 | 0.79 | Dissolved Oxygen (DO) |
| Temperature | °C | 18 | 0.50 | Temperature |
| NaOCl dose | mg $L^{-1}$ | 2.0 | 1.90 | NaOCl dose |

Residual iron concentrations were determined using the 1,10-phenanthroline colorimetric method with a DR/2010 spectrophotometer (Hach, USA) at the Homs Water Establishment Laboratory. All experimental conditions were tested in triplicate (n = 3), and results are reported as mean ± standard deviation (SD).

Iron concentrations were measured using a Hach UV/VIS Spectrophotometer DR 2010 following the standard phenanthroline method. According to the manufacturer's specifications, the method detection limit (MDL) for dissolved iron is approximately 0.02 mg/L, with a reliable quantification range extending to several mg/L depending on sample dilution. This detection limit is well below the regulatory guideline value for iron in drinking water (0.3 mg/L), providing sufficient sensitivity to evaluate treatment performance and regulatory compliance. All reported iron concentrations, including values below 0.1 mg/L, exceed the MDL of the instrument and are therefore considered analytically reliable [40].

### 3.2. Jar Test Procedure

Jar test experiments were conducted in the Environmental Engineering Laboratory at Homs University in accordance with ASTM D2035 guidelines. The operational parameters were as follows: rapid mixing (coagulation) at 150 rpm for 2 min, slow mixing (flocculation) at 20 rpm for 15 min, and a settling period of 90 min. Following sedimentation, samples were filtered under gravity through a 0.45-µm pore-size filter paper. Residual iron concentrations were determined using a spectrophotometer.

#### 3.2.1. Effect of pH on the Efficiency of Sodium Hypochlorite Oxidation

The objective of these experiments was to determine the optimal sodium hypochlorite dosage as a function of solution pH. The characteristics of the raw water used were as follows: iron concentration of 1.5 mg/L and temperature of 18 °C. Experiments were performed using a standard jar test apparatus. Samples were subjected to

rapid mixing at 150 rpm for 2 min, followed by slow mixing at 20 rpm for 15 min, in accordance with ASTM D2035. The pH of the samples was adjusted to values of 4, 5, 6, 7, 8, 9, and 10 using sodium hydroxide (NaOH) and sulfuric acid ($H_2SO_4$). A calibrated pH probe was immersed in each beaker to continuously monitor pH during adjustment.

Subsequently, sodium hypochlorite (NaOCl) was added at doses of 1.5, 3.0, 4.5, and 6.0 mg/L. After rapid mixing at 150 rpm for 2 min and a 15-min contact time, the samples were allowed to settle for 90 min. The supernatant was then filtered and analyzed for residual iron concentration. The relationship between sodium hypochlorite dosage and residual iron concentration was evaluated at each pH level. Each experiment was conducted in duplicate, and the average values were obtained.

### 3.2.2. Effect of Dissolved Oxygen on Iron Removal

To investigate the effect of dissolved oxygen (DO) on iron oxidation, water samples were aerated using an air pump. Air was introduced into four 1-L cylinders to increase DO concentrations. The raw water had an initial DO concentration of 3 mg/L and a pH of 7.3.

Dissolved oxygen levels were monitored continuously during aeration. Aeration was terminated once DO concentrations of 4, 5, 6, and 7 mg/L were achieved, after which the samples were allowed to settle for 90 min. The approximate aeration times and corresponding air volumes required to reach each DO level were as follows: 3 min (10.5 L air/L water) for 4 mg/L, 8 min (28 L/L) for 5 mg/L, 11 min (38.5 L/L) for 6 mg/L, and 16 min (56 L/L) for 7 mg/L. Aeration beyond 16 min was ineffective due to temperature-induced changes in oxygen solubility and saturation limits. During the settling period, samples were collected from the surface every 10 min, filtered, and analyzed for residual iron concentration.

### 3.2.3. Effect of pH Adjustment on Aeration Efficiency

The influence of pH adjustment before aeration on iron removal efficiency was evaluated at different dissolved oxygen levels. The initial characteristics of the raw water were pH 7.0 and DO 3 mg/L. A series of experiments was conducted at DO concentrations of 3, 5, and 7 mg/L. At the same time, the pH of the raw water was adjusted to 6.5-8.5 in accordance with the Syrian Standard Specification for Drinking Water No. 45 (2007). Sodium hydroxide was used to increase pH, while sulfuric acid was used to decrease pH. Results indicated that aeration efficiency increased with increasing pH, with a particularly pronounced improvement observed in the pH range of 6.5 to 7.5.

### 3.2.4. Combined Chemical and Aeration Oxidation Treatment

A combined treatment approach incorporating chemical oxidation and aeration was evaluated for iron removal. Sodium hypochlorite was applied at 1.5, 3.0, and 4.5 mg/L, followed by aeration to raise dissolved oxygen to 4, 5, and 6 mg/L. After treatment, samples were allowed to settle for 60 min. Residual iron concentrations were measured every 10 min following filtration.

### 3.2.5. Effect of Oxidant Dose at Varying Iron Concentrations

Additional experiments were conducted to examine the effect of sodium hypochlorite dosage on iron removal at different initial iron concentrations. In all experiments, the pH of the raw water was maintained at 7.5 and the dissolved oxygen concentration was fixed at 3 mg/L. The only variable parameter was the initial iron concentration in the raw water. Five experimental sets were performed under these conditions. The detailed experimental parameters are summarized in Table 2, and the conceptual framework of the study (Figure 1).

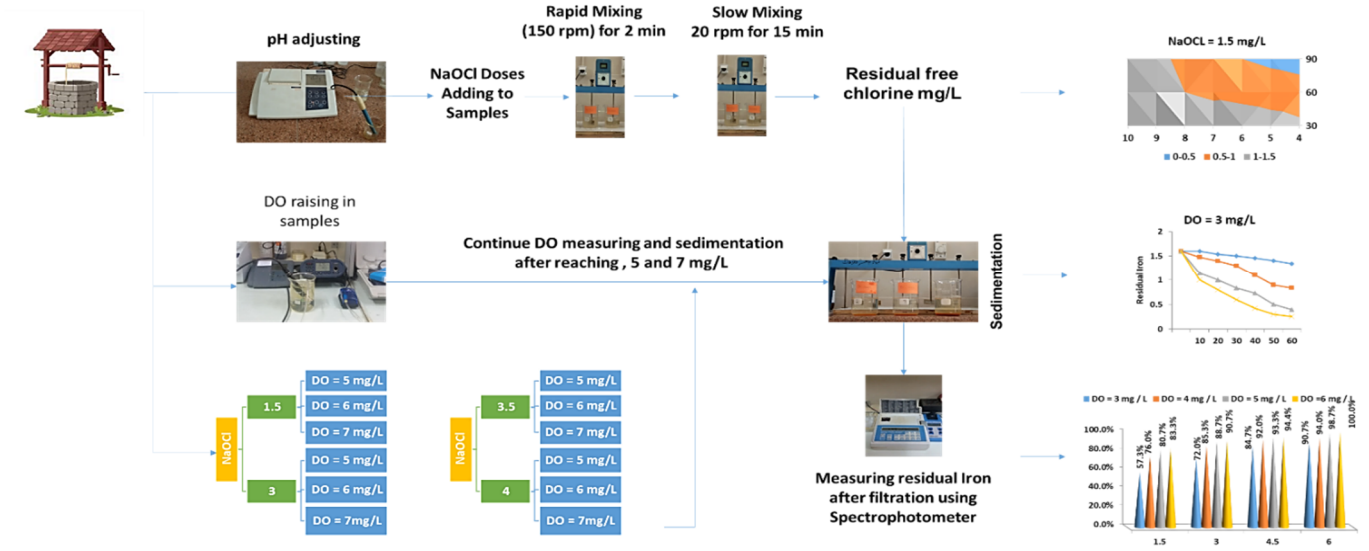


**Figure 1.** Conceptual framework of research

**Table 2.** Conditions for the five sets of Jar Test experiments

| Set | Fe (mg/L) | NaOCl (mg/L) | pH | Temperature (°C) | DO (mg/L) |
|---|---|---|---|---|---|
| 1 | 1.5 ± 0.1 | 1.5, 3.0, 4.5, 6.0 | 7.0 ± 0.3 | 18 ± 2 | 4.0 ± 0.2 |
| 2 | 1.5 ± 0.1 | – | 7.0 ± 0.3 | 18 ± 2 | 4.0, 5.0, 6.0, 7.0 |
| 3 | 1.5 ± 0.1 | – | 6.5, 7.0, 7.5, 8.0 | 18 ± 2 | 3.0, 5.0, 7.0 |
| 4 | 1.5 ± 0.2 | 1.5, 3.0, 4.5, 6.0 | 7.0 ± 0.3 | 18 ± 2 | 3.0, 4.0, 5.0, 6.0 |
| 5 | 1.0, 1.5, 2.0, 2.5 ± 0.1 | 1.5, 3.0, 4.5, 6.0 | 7.0 ± 0.3 | 18 ± 2 | 4.0 ± 0.2 |

### 3.3. Gene Expression Programming (GEP)

Cândida Ferreira introduced Gene Expression Programming (GEP) as an evolutionary algorithm that combines the representational strengths of genetic algorithms (GAs) and genetic programming (GP) [41]. Unlike conventional GAs, which employ fixed-length binary or real-valued chromosomes, and GP, which directly evolves tree-structured programs, GEP utilizes fixed-length linear chromosomes (genotype) that are subsequently expressed as non-linear expression trees (phenotype).

In GEP, each chromosome consists of one or more genes, and each gene is divided into a head and a tail. The head may contain both functions and terminals, whereas the tail contains only terminals, ensuring that every gene is translated into a syntactically valid expression tree. Through a decoding process known as Karva notation, chromosomes are expressed as one or more expression trees, which are then evaluated according to a predefined fitness function.

The evolutionary process of GEP follows standard evolutionary computation procedures, including population initialization, chromosome decoding, fitness evaluation (e.g., regression error or prediction accuracy), selection of superior individuals, and the application of genetic operators such as mutation, crossover, transposition, and gene recombination to generate successive generations [36].

One of the principal advantages of GEP is its interpretability. Because the final model is represented as an explicit mathematical expression, the resulting relationships can be written in closed form, enabling direct physical or mechanistic interpretation. This contrasts with black-box models such as artificial neural networks (ANNs) and support vector machines (SVMs). Consequently, GEP is particularly well-suited for symbolic regression, system modeling, and engineering optimization problems where transparent functional relationships are desirable.

In this study, GEP was selected due to its ability to generate explicit mathematical models, especially when dealing with relatively small datasets compared to other machine learning approaches. A total of 56 data samples were used, of which 70% were randomly assigned to the training set and 30% to the test set using the GEP software [37].

**Table 3.** GEP control parameters used in study

| Category | Parameter | Values |
|---|---|---|
| General settings | Function set | +, −, ×, ÷, √, exp, ln, log, $10^x$ |
| | Fitness function | RMSE |
| | Linking function | + |
| | Data type | Floating-point |
| | Maximum complexity | 10 |
| Chromosome structure | Number of chromosomes | 600 |
| | Head size | 7 |
| | Tail size | 3 |
| | Constants per gene | 10 |
| Genetic operators | Mutation rate | 0.0014 |
| | Inversion rate | 0.0055 |
| | IS the transposition rate | 0.0055 |
| | RIS transposition rate | 0.0055 |
| | One-point recombination rate | 0.0028 |
| | Two-point recombination rate | 0.0028 |
| | Gene recombination rate | 0.0028 |
| | Uniform recombination rate | 0.0076 |

To evaluate the performance of the developed predictive model, this study employs three primary statistical indicators. Root Mean Squared Error (RMSE) quantifies the square root of the average of the squared differences between the predicted values and the observed (actual) values. This metric assigns greater weight to larger errors, making it particularly sensitive to significant deviations.

$$RMSE = \sqrt{\frac{1}{n}\sum_{i=1}^{n}\left(P_{obs,i} - P_{pre,i}\right)^2} \quad (1)$$

The Correlation Coefficient (R), commonly known as the Pearson correlation coefficient, measures the strength

and direction of the linear relationship between observed and predicted values.

$$R = \frac{\sum_{i=1}^{n}(P_{obs,i} - \overline{P}_{obs})(P_{pre,i} - \overline{P}_{pre})}{\sqrt{\sum_{i=1}^{n}(P_{obs,i} - \overline{P}_{obs})^2 \sum_{i=1}^{n}(P_{pre,i} - \overline{P}_{pre})^2}} \quad (2)$$

Mean Absolute Error (MAE) represents the average magnitude of the absolute differences between the predicted values and the observed values. Unlike RMSE, this metric treats all errors uniformly without disproportionately emphasizing larger deviations.

$$MAE = \frac{1}{n}\sum_{i=1}^{n}|P_{obs,i} - P_{pre,i}| \quad (3)$$

where:

$n$ : The total number of data samples;
$P_{obs}$ : The observed (actual) values;
$P_{pre}$ : The predicted values generated by the model;
$\overline{P}_{obs}$ : The mean of the observed data, and
$\overline{P}_{pre}$ : The mean of the predicted data.

## 4. RESULTS

### 4.1. Effect of pH Variation on the Efficiency of Sodium Hypochlorite

The chemical treatment of iron-containing water primarily aims to oxidize dissolved iron with an appropriate oxidizing agent, thereby transforming it into insoluble, readily removable compounds. Numerous studies have investigated various chemical oxidants for this purpose; however, most of the existing literature does not explicitly report the dosage levels of sodium hypochlorite used in iron removal processes. This lack of detailed dosage information highlights the need for systematic evaluation of sodium hypochlorite performance across different pH conditions and concentration ranges.

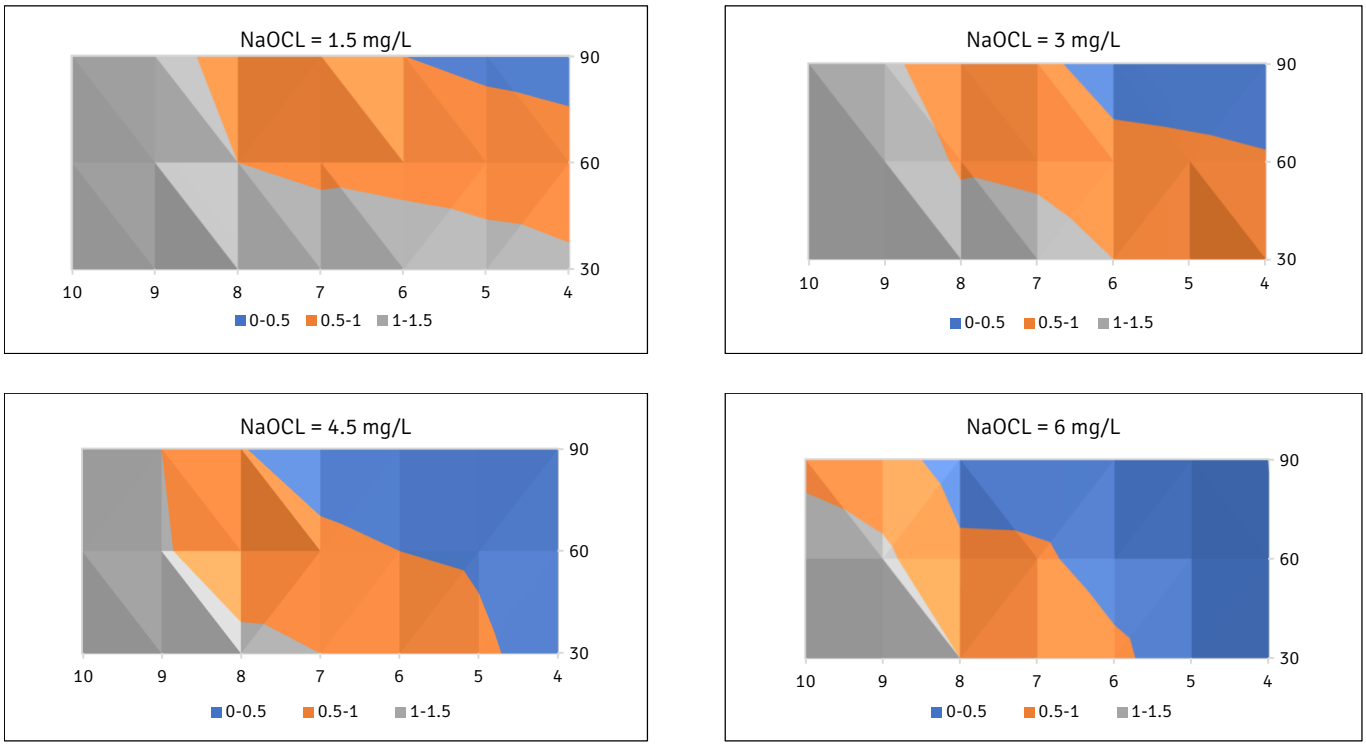


**Figure 2.** Iron residuals according to NaOCl and pH levels

The inclusion of acidic pH conditions in the experimental design was primarily intended to broaden the parameter space and capture the full non-linear response of iron oxidation to pH variation when sodium hypochlorite is employed as the oxidizing agent. Expanding the pH range enhances the robustness of the resulting predictive model by enabling more reliable estimation of model coefficients and a more accurate representation of chlorine speciation effects. Although pH values below the typical drinking-water range are not intended for operational application, they provide critical information for model calibration and for elucidating the sensitivity of iron removal efficiency to oxidant chemistry.

**Table 4.** Residual free chlorine concentrations at different NaOCl and pH values

| Sample (pH) | NaOCl Dose | | | |
|---|---|---|---|---|
| | 6 mg/L | 4.5 mg/L | 3 mg/L | 1.5 mg/L |
| 6 | 0.45 | 0.29 | 0.20 | 0.18 |
| 7 | 0.50 | 0.32 | 0.20 | 0.20 |
| 8 | 0.52 | 0.40 | 0.23 | 0.22 |

The experimental results clearly demonstrate that the effectiveness of sodium hypochlorite (NaOCl) in removing iron from groundwater is strongly pH-dependent. A maximum iron removal efficiency of 99% was achieved at pH 4 with a NaOCl dosage of 6 mg/L, whereas the efficiency decreased to 40% at pH 10 under the same dosage. This trend was consistently observed across all tested NaOCl concentrations, indicating that acidic conditions are more favorable for iron removal using this treatment approach. The residual free chlorine concentrations measured at different NaOCl dosages and pH levels (Table 4) support this observation.

### 4.2. Effect of Dissolved Oxygen Variation on Iron Removal Efficiency

Oxidation by aeration is one of the most widely used methods for removing dissolved iron from water. This process can be implemented using several techniques, including spray aeration and direct air injection. Previous studies have consistently shown that increasing the dissolved oxygen (DO) concentration enhances iron oxidation and, consequently, improves removal efficiency. In the present study, the relationship between pH, DO concentration, and iron removal efficiency was investigated.

**Table 5.** Effect of changing the value of dissolved oxygen on iron removal

| DO (mg/L) | Iron concentration in raw water (mg/L) | Deposition time (min) | | |
|---|---|---|---|---|
| | | 30 | 60 | 90 |
| | | Concentration of residual iron in water after treatment (mg/L) | | |
| 4 | 1.5 | 1.20 | 0.80 | 0.75 |
| 5 | 1.5 | 0.97 | 0.72 | 0.51 |
| 6 | 1.5 | 0.93 | 0.52 | 0.32 |
| 7 | 1.5 | 0.75 | 0.40 | 0.26 |

Table 5 summarizes the variation in residual iron concentration as a function of DO level, sedimentation time, and initial iron concentration. As shown in the table, increasing the DO concentration from 4 to 6 mg/L resulted in a substantial decrease in residual iron concentration, from 0.75 mg/L to 0.32 mg/L, in compliance with the permissible limit specified by the Syrian Standard Specification for Drinking Water No. (45) of 2007 was achieved after approximately 30 minutes of sedimentation. Under these conditions, an air-to-water ratio of approximately 38.5 L of air per liter of water was required.

Further increases in DO concentration to 7 mg/L led to only marginal reductions in residual iron concentration, as indicated in Table 5. Although improved removal was observed, the associated increase in aeration intensity would result in higher electrical energy consumption and operational costs. Consequently, the incremental benefit of raising the DO concentration beyond 6 mg/L is not economically justified.

To facilitate clearer interpretation of these trends, Figure 3 illustrates the percentage of iron removal as a function of DO concentration. The figure corroborates the tabulated results by demonstrating a sharp increase in removal efficiency with increasing DO up to 6 mg/L, followed by a plateau at higher DO values. This behavior confirms that a DO concentration of 6 mg/L represents an optimal operating condition, balancing effective iron removal with energy efficiency.

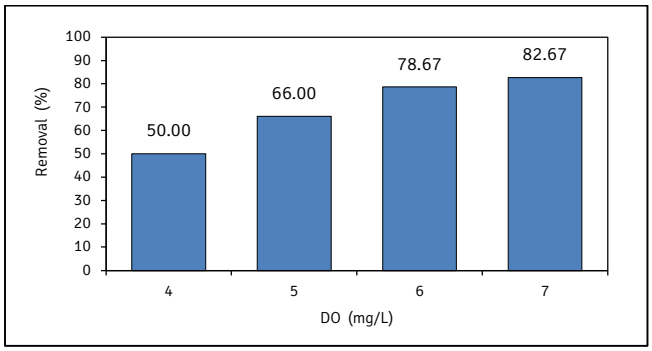


**Figure 3.** Percentage of iron removal according to the DO value

The percentage of iron removal increased with increasing dissolved oxygen (DO) concentration, which reflects the fundamental objective of the aeration process. At a DO concentration of 7 mg/L, the iron removal efficiency reached 82.67%. In contrast, at a DO concentration of 4 mg/L, the residual iron concentration after laboratory filtration was 0.26 mg/L, corresponding to approximately 50% removal efficiency. Previous studies have shown that aeration may affect the pH of treated water through oxidation reactions. Accordingly, pH was monitored in this study by measuring the pH after aeration was terminated at a DO concentration of 5 mg/L. The temporal change in pH during the oxidation process was analyzed (Figure 4).

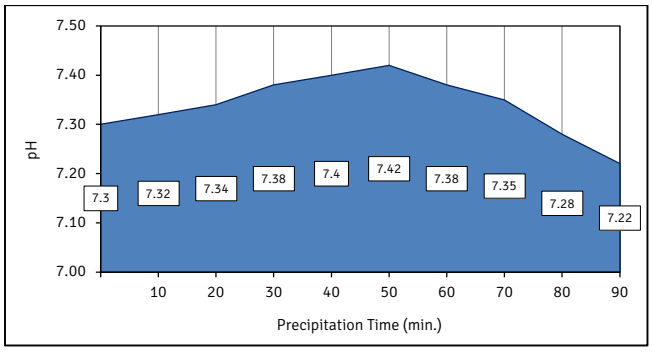


**Figure 4.** Change in pH during the oxidation process.

The pH increased slightly during the intermediate stage of the oxidation process and returned to its initial level after approximately 90 minutes. This temporary increase was minor and did not adversely affect water quality standards or treatment performance. In addition, longer sedimentation times were found to enhance iron removal

efficiency. As shown (Table 5), residual iron concentrations consistently decreased as the deposition time increased from 30 to 90 minutes. This trend can be attributed to the time-dependent formation, aggregation, and gravitational settling of ferric hydroxide particles following iron oxidation.

### 4.3. Effect of pH Variation of Raw Water on Aeration Treatment Efficiency

The treatment performance at pH 7.5 and pH 8 shows relatively similar trends, whereas at pH 6.5 the residual iron concentration remains noticeably higher. At pH 6.5, the residual iron concentration after 60 minutes of aeration is approximately 1.35 mg/L, while at pH 8 it decreases to about 0.38 mg/L over the same duration. In general, for all tested pH values, the residual iron concentration gradually decreases with increasing aeration time, indicating that higher pH levels enhance iron oxidation and subsequent removal.

Figure 5 illustrates the effect of pH variation on residual iron concentration at dissolved oxygen (DO) levels of 3, 5, and 7 mg/L. The horizontal axis represents sedimentation time, while the vertical axis indicates the remaining iron concentration after sedimentation and filtration. The results show a significant reduction in iron concentration within the first 20 minutes of sedimentation, followed by a more gradual decline. At a DO concentration of 5 mg/L, the iron removal efficiency reaches approximately 80% at pH 7.5, corresponding to a residual iron concentration of about 0.3 mg/L. Further increases in pH beyond this level do not result in a substantial improvement in removal efficiency.

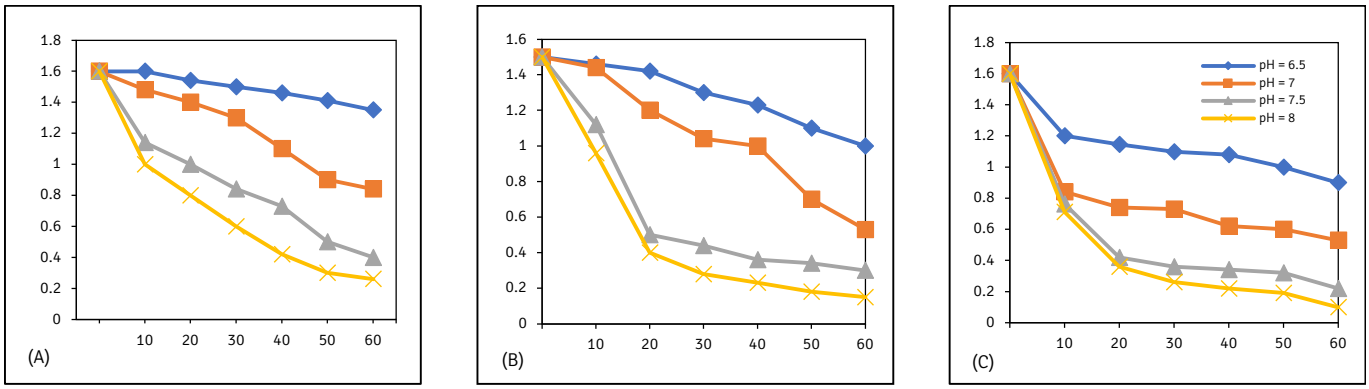


**Figure 5.** Effect of Changing pH on the Residual Iron Concentration (DO=3, 5, 7 mg/L)

### 4.4. Combined Treatment of Iron by Chemical Oxidation and Aeration Oxidation

The results clearly demonstrate that an increase in the initial iron concentration in raw water corresponds to a higher sodium hypochlorite dose required to achieve effective iron reduction. At lower oxidant doses, higher initial iron concentrations result in elevated residual iron levels, indicating insufficient oxidation. Conversely, increasing the NaOCl dose enhances iron removal efficiency across all tested iron concentrations.

The combined treatment of aeration and sodium hypochlorite (NaOCl) proved economically and technically effective for iron removal. At a dissolved oxygen (DO) concentration of 4 mg/L, a NaOCl dose of 3 mg/L achieved an iron removal efficiency of 85.33%, reducing residual iron to 0.22 mg/L. Experimental results further showed that higher DO levels reduced the NaOCl dose required for effective treatment, confirming a synergistic effect between oxygenation and chemical oxidation in the aeration–chlorination sequence.

The achieved removal efficiency is comparable to values reported in the literature, such as 93% with chlorination and rapid sand filtration [34] and up to 88% with granular activated carbon (GAC) filtration [42]. Unlike adsorption- or filtration-dominated systems, the present study focuses on oxidation-driven iron removal, highlighting the advantage of NaOCl's strong, pH-dependent oxidizing capacity when combined with aeration to minimize chemical demand.

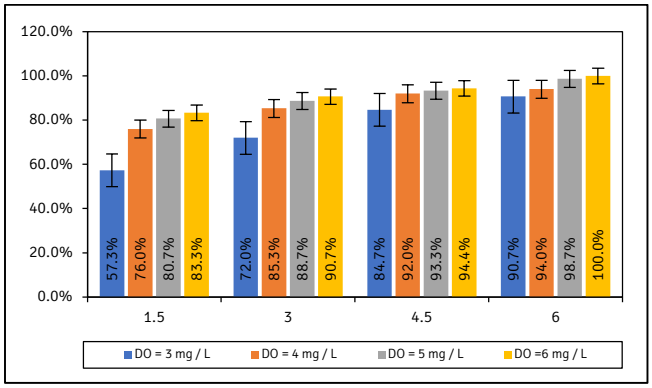


**Figure 6.** Effect of varying sodium hypochlorite dose on residual iron concentration at different initial iron concentrations in raw water.

Differences in treatment mechanisms, influent water quality, and operational conditions, including TOC levels, contact time, and system configuration, constrain direct comparison with previous studies. While reported efficiencies appear similar, variations likely reflect differing process designs rather than intrinsic

performance. By systematically controlling and reporting pH, DO, treatment sequence, and influent characteristics, this study provides context-specific, reproducible evidence that combined NaOCl oxidation and aeration are an effective and sustainable approach for groundwater iron removal.

### 4.5. Effect of Oxidant Dose Variation with Changes in Raw Water Iron Concentration

Figure 7 illustrates the results of experiments conducted to evaluate the effect of varying sodium hypochlorite doses on iron removal at different initial iron concentrations in raw water. The figure shows the residual iron concentration after treatment with NaOCl at 1.5, 3.0, 4.5, and 6.0 mg/L.

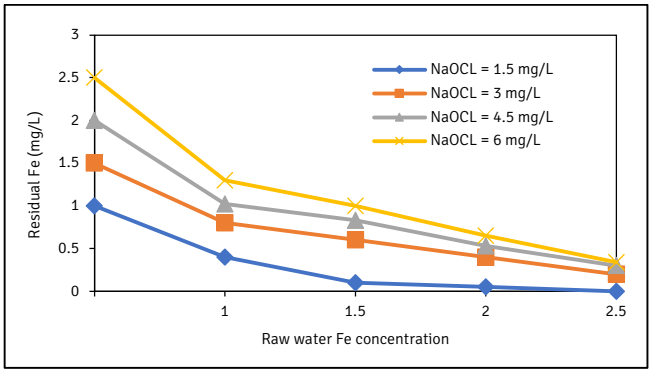


**Figure 7.** Effect of varying sodium hypochlorite dose on residual iron concentration at different initial iron concentrations in raw water.

The results clearly demonstrate that an increase in the initial iron concentration in raw water corresponds to a higher sodium hypochlorite dose required to achieve effective iron reduction. At lower oxidant doses, higher initial iron concentrations result in elevated residual iron levels, indicating insufficient oxidation. Conversely, increasing the NaOCl dose enhances iron removal efficiency across all tested iron concentrations. This trend reflects the increasing oxidant demand associated with higher ferrous iron levels and is consistent with the stoichiometric and kinetic requirements of iron oxidation reactions. The findings emphasize the importance of adjusting the oxidant dosage to account for variations in influent iron concentration to ensure effective, efficient treatment performance.

### 4.6. Cost of Chemical Oxidation Treatment

The chemical oxidation process was evaluated for groundwater with an average iron concentration of 1.5 mg/L, a pH of 7.5, and a temperature of 18°C. Laboratory optimization experiments indicated that an effective sodium hypochlorite (NaOCl) dose of 4.5 mg/L was required to achieve complete oxidation of dissolved ferrous iron under these conditions. Considering that the commercial sodium hypochlorite solution used in this study had a concentration of 3%, corresponding to approximately 30 g/L of available chlorine, this dose is equivalent to a solution consumption of 0.15 mL/L, or 0.15 L per cubic meter of treated groundwater. Based on a local market survey, the unit price of sodium hypochlorite was 7000 Syrian Pounds (SYP) per liter. Accordingly, the chemical cost of treating 1 cubic meter of groundwater using chemical oxidation alone was estimated at 1050 SYP/m³, corresponding to approximately 0.095 USD/m³ (1 USD = 11,000 SYP).

### 4.7. Cost of Aeration Oxidation Treatment

The results of the aeration experiments demonstrated that efficient iron removal through aeration required increasing the dissolved oxygen concentration to approximately 6 mg/L. Achieving this oxygen level required supplying approximately 38.5 liters of air per liter of water, equivalent to 38.5 cubic meters of air per cubic meter of treated water. Aeration was performed using an air blower with a nominal capacity of 500 m³/h and a power consumption of 18.5 kW. Under steady operating conditions, this corresponds to an air delivery rate of approximately 27 m³ per kilowatt-hour of electricity. Based on these parameters, the energy demand for treating one cubic meter of groundwater was estimated at 1.43 kWh. Considering the local electricity tariff of 1,700 SYP per kilowatt-hour, the operational cost of aeration oxidation was calculated to be approximately 2,431 SYP/m³, equivalent to about 0.22 USD/m³.

### 4.8. Cost of Combined Treatment (Pre-Chlorination Followed by Aeration)

The combined treatment approach, consisting of low-dose pre-chlorination followed by aeration, demonstrated a significant reduction in overall energy consumption. The addition of 3 mg/L sodium hypochlorite partially oxidized ferrous iron, thereby reducing the dissolved oxygen requirement during the subsequent aeration stage. In this case, the dissolved oxygen concentration only needed to be increased from 3 mg/L to 4 mg/L, which corresponded to an air supply of approximately 10.5 liters of air per liter of water, or 10.5 m³ of air per cubic meter of treated water. This reduced air demand resulted in an energy consumption of approximately 0.37 kWh/m³. At an electricity cost of 1,700 SYP per kilowatt-hour, the aeration cost was estimated at 693 SYP per m³. The chemical cost of pre-chlorination was calculated at 700 SYP/m³, based on a sodium hypochlorite consumption rate of 0.1 L/m³. Consequently, the total operational cost of the combined treatment process was estimated at 1,393 SYP/m³, corresponding to approximately 0.13 USD/m³.

Table 6 summarizes the operational costs associated with the three investigated iron oxidation treatment strategies. Among the evaluated options, aeration alone exhibits the highest cost due to its substantial energy demand. Chemical oxidation using sodium hypochlorite

represents the lowest standalone cost; however, it relies entirely on continuous chemical consumption. The combined pre-chlorination and aeration approach provides an optimal balance, reducing energy requirements by approximately 74% compared to aeration alone, while maintaining a moderate total operational cost.

**Table 6.** Comparison of operational costs for different iron oxidation treatment methods

| Treatment Method | NaOCl Dose (mg/L) | NaOCl Consumption (L/m³) | Energy Consumption (kWh/m³) | Cost (SYP/m³) | Cost (USD/m³)* |
|---|---|---|---|---|---|
| Chemical Oxidation (NaOCl) | 4.5 | 0.15 | – | 1,050 | 0.095 |
| Aeration Oxidation | – | – | 1.43 | 2,431 | 0.22 |
| Combined treatment (pre-chlorination + aeration) | 3.0 | 0.10 | 0.37 | 1,393 | 0.13 |

*Conversion rate: 1 USD = 11,000 SYP (Source: www.xe.com, 5 January 2026)

Figure 8 presents a comparative evaluation of treatment cost and iron removal efficiency for the three investigated methods: chemical oxidation (CH-O), aeration oxidation, and the combined treatment (pre-chlorination followed by aeration). The aeration oxidation method exhibits the highest operational cost (2,431 SYP/m³) and the lowest removal efficiency (78.7%), primarily due to its high energy demand. In contrast, chemical oxidation achieves a high removal efficiency (87.5%) at the lowest cost (1,050 SYP/m³), owing to the exclusive reliance on chemical dosing. The combined treatment method demonstrates a favorable balance between cost and performance, achieving the highest removal efficiency (89%) while reducing the total treatment cost to 1,393 SYP/m³.

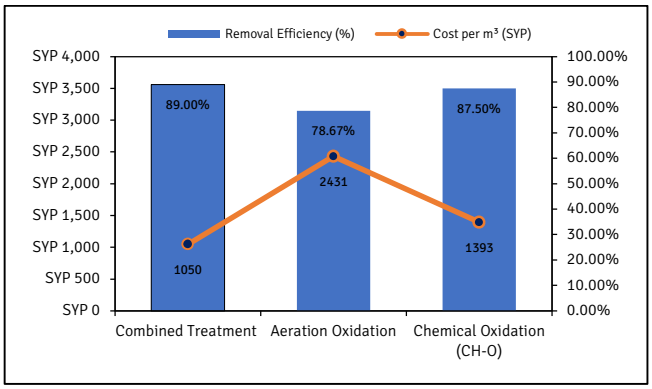


**Figure 8.** Comparison of treatment cost and iron removal efficiency for chemical oxidation (CH-O), aeration oxidation, and combined treatment methods.

The combined treatment approach, involving pre-chlorination followed by aeration, offers a technically and economically balanced alternative. By applying a relatively low NaOCl dose before aeration, the required dissolved oxygen level is significantly reduced, thereby decreasing energy consumption. Consequently, the total treatment cost is reduced by approximately 42.7% compared to aeration oxidation alone, while achieving the highest iron removal efficiency (89%). These findings demonstrate that the combined method represents an optimal compromise between treatment efficiency, operational cost, and energy demand for groundwater iron removal.

### 4.9. Gene Expression Programming (GEP) Model

The performance of the Gene Expression Programming (GEP) model was evaluated to determine its ability to predict the required sodium hypochlorite (NaOCl) dosage for iron oxidation. The model was implemented in GenXPro and assessed across different chromosome configurations, with the GEP control parameters applied during model development and optimization (Table 7).

**Table 7.** GEP control parameters used for model development and optimization

| Parameter | GEP 1-1 | GEP 1-2 | GEP 2-1 | GEP 2-2 |
|---|---|---|---|---|
| Function set | +, −, ×, ÷, √, exp, ln, log, $10^x$ | +, −, ×, ÷, √, exp, ln, log, $10^x$ | +, −, ×, ÷, √, exp, ln, log, $10^x$ | +, −, ×, ÷, √, exp, ln, log, $10^x$ |
| Number of chromosomes | 500 | 600 | 800 | 900 |
| Fitness function | RMSE | RMSE | RMSE | RMSE |
| Linking function | + | + | + | + |
| Mutation rate | 0.00138 | 0.01 | 0.00138 | 0.01 |
| Head size | 8 | 7 | 8 | 7 |

**Table 8.** The performance of the optimal model

| Dataset | Data points | $R^2$ | RMSE | MAE |
|---|---|---|---|---|
| Training set | 39 | 0.95 | 0.32 | 0.226 |
| Testing set | 17 | 0.93 | 0.36 | 0.320 |

Among the tested configurations, the model incorporating 800 chromosomes exhibited the best overall performance. This configuration achieved coefficients of determination ($R^2$) of 0.95 and 0.93 for the training and testing datasets, respectively, accompanied by low RMSE and MAE values. These results indicate strong predictive accuracy and good generalization capability. The structural

representation of the optimal GEP model, expressed as a gene-expression tree (Figure 9).

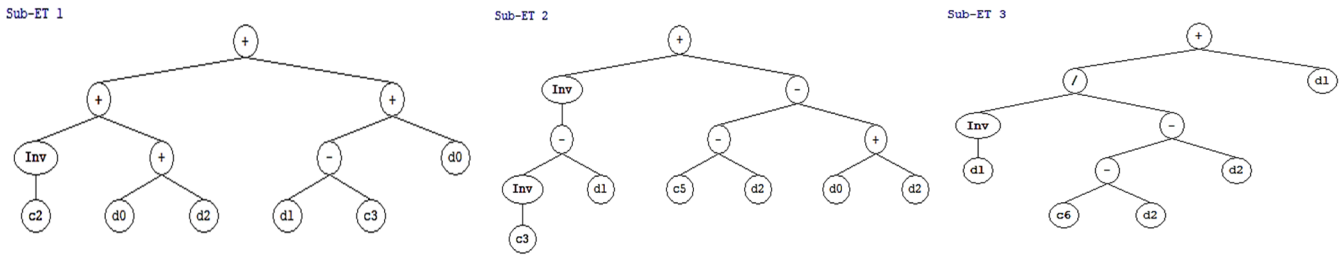


**Figure 9.** Gene-expression tree of the optimal GEP model

$$NAOCl = \frac{1}{3.0722157} + pH + 2Fe - 7.973099 + \frac{1}{\frac{1}{1.8349620}} + 6.6817344 + \frac{\frac{1}{Fe}}{9.5449601 - 2DO} \quad (4)$$

**Table 9.** Variables and constants of the derived GEP model equation

| $d_0$ | $d_1$ | $d_2$ | C1C2 | C1C3 | C2C5 | C2C3 | C3C6 |
|---|---|---|---|---|---|---|---|
| pH | Fe | DO | 3.0755157 | 7.973099 | 6.6817344 | 1.8349620 | 9.5449601 |

The optimal GEP model yields a mathematical expression that relates NaOCl dosage to the input variables pH, dissolved oxygen (DO), and influent iron concentration (Fe). The constants and variables defining this equation (Table 9), form the basis for the quantitative prediction of oxidant demand under varying operational conditions

Model validation was performed by comparing the NaOCl dosages predicted by the GEP model with experimentally measured values (Figure 11). A strong agreement between the two datasets is observed, with prediction errors ranging from 0 to 1.3. This close correspondence confirms the GEP model's high accuracy in estimating NaOCl requirements.

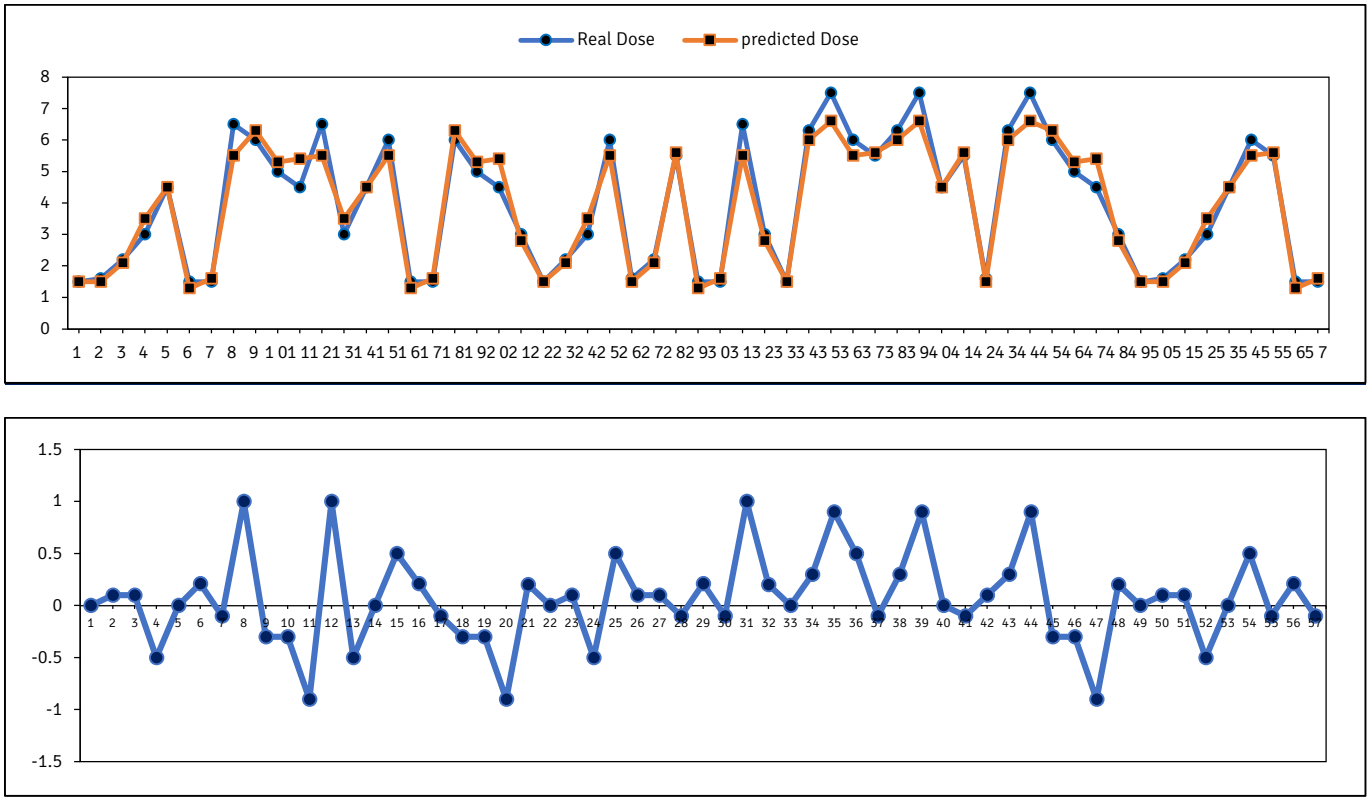


**Figure 10.** Comparison between predicted and experimental NaOCl dosages

The predictive reliability of the model was further examined using a scatter plot of observed versus predicted NaOCl dosages (Figure 11). The majority of data points are clustered near the 1:1 reference line, demonstrating a strong correlation and indicating that the GEP model maintains robust predictive performance across the investigated range of operating conditions.

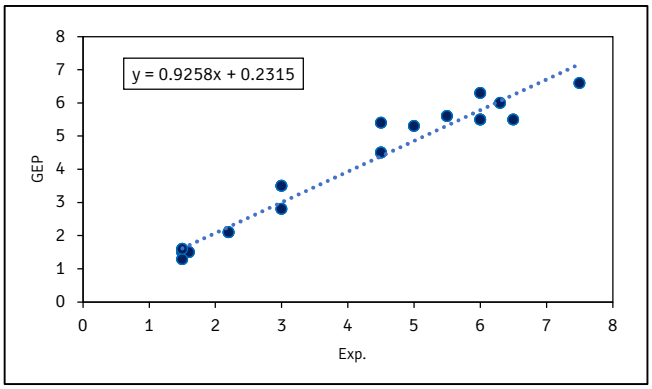


**Figure 11.** Observed versus predicted NaOCl dosages using the GEP Model

To evaluate the influence of individual input variables on model output, a sensitivity analysis was conducted. The results (Figure 12) indicate that pH and DO are the dominant variables, contributing 35.6% and 35.5%, respectively, to the overall sensitivity, while influent iron concentration accounts for 28.9%. These findings suggest that oxidant demand is primarily controlled by physicochemical reaction conditions rather than iron concentration alone.

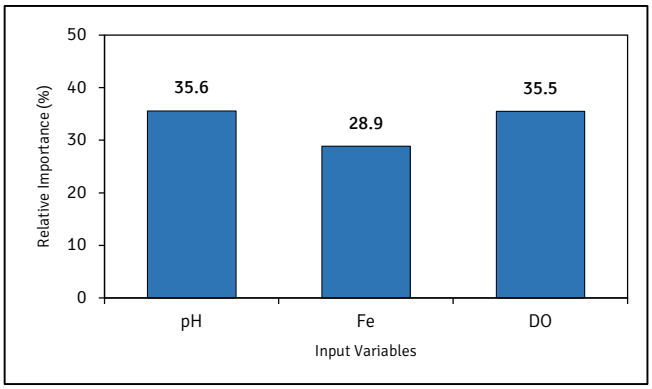


**Figure 12.** Sensitivity analysis of input variables in the GEP Model for NaOCl dosage prediction.

From a mechanistic perspective, these results are consistent with established iron oxidation chemistry. The strong influence of pH reflects its critical role in controlling chlorine speciation ($HOCl/OCl^-$) and iron oxidation kinetics. Meanwhile, the substantial contribution of DO highlights the importance of oxygen availability in facilitating ferrous iron oxidation and subsequent ferric hydroxide precipitation. The comparatively lower sensitivity associated with influent iron concentration indicates that, within the investigated range, reaction conditions exert a greater control on NaOCl demand than the absolute iron mass.

## 5. DISCUSSION

The experimental results clearly demonstrate a strong dependence of iron removal efficiency on pH when sodium hypochlorite (NaOCl) is employed as the oxidizing agent. Maximum removal efficiency of 99% was achieved at pH 4, consistent with the well-established chemistry of chlorine speciation in aqueous systems. As reported by Deborde and von Gunten [8], the oxidative capacity of chlorine is governed by the pH-dependent equilibrium between hypochlorous acid (HOCl) and the hypochlorite ion ($OCl^-$). Under acidic to neutral conditions, HOCl predominates and exhibits a substantially higher oxidation potential than $OCl^-$, thereby enabling rapid and efficient oxidation of ferrous iron ($Fe^{2+}$) to ferric iron ($Fe^{3+}$). The superior performance observed at pH 4 in this study can therefore be attributed to the dominance of HOCl, which accelerates iron oxidation and promotes subsequent precipitation as ferric hydroxide.

Although similar trends have been reported in previous studies, much of the existing literature has focused on neutral to slightly alkaline conditions relevant to drinking water treatment rather than explicitly identifying peak oxidation efficiency under acidic conditions. While such low pH values are not directly applicable to full-scale drinking water systems due to regulatory constraints and corrosion concerns [43], these findings nonetheless provide valuable mechanistic insights into oxidation processes and underscore the critical role of pH control in optimizing NaOCl dosing. Fundamental studies have shown that hypochlorous acid (HOCl), which predominates at pH values below 7.5, is a stronger and more kinetically reactive oxidant than the hypochlorite ion ($OCl^-$), thereby explaining the enhanced oxidation efficiency observed under acidic conditions [44]. At the same time, under neutral conditions (pH 7–7.5), relatively high removal efficiencies of approximately 85% were still achieved at moderate NaOCl doses, consistent with previously reported chlorination-based iron removal studies that document effective performance within the neutral pH range commonly employed in conventional water treatment applications [45].

In addition to pH, the aeration experiments further confirmed the significant role of dissolved oxygen (DO) in enhancing iron removal efficiency. Increasing DO concentrations from 3 to 6 mg/L reduced residual iron levels to approximately 0.32 mg/L, whereas further increases to 7 mg/L resulted in only marginal improvements, indicating diminishing returns with respect to additional energy input. This observation is consistent with classical iron oxidation kinetics described by McPeak and Aronovitch [17], who demonstrated that the rate of iron oxidation is directly proportional to the dissolved oxygen concentration and to the square of the

hydroxide ion concentration. Compared with values reported in the literature, the DO levels required in this study to meet regulatory limits were comparable or slightly lower. This outcome may be attributed to the relatively moderate initial iron concentration (approximately 1.5 mg/L), controlled laboratory conditions, and sufficient settling time that allowed complete precipitation and removal of ferric hydroxides. Although aeration is an effective, chemical-free treatment approach, these results underscore that its performance is highly sensitive to operational conditions, and excessive aeration yields diminishing improvements in removal efficiency while substantially increasing energy consumption and operational costs.

The combined application of chemical oxidation and aeration—particularly the sequence of pre-chlorination followed by aeration—constitutes one of the most significant and novel contributions of this study. Although combined treatment systems are commonly employed, the influence of treatment sequence has rarely been explicitly examined in previous research. Most studies emphasize overall removal efficiency without differentiating between pre-chlorination followed by aeration and aeration followed by chlorination. The results presented here clearly demonstrate that pre-chlorination followed by aeration yields superior performance, achieving iron removal efficiencies of 85–89% at relatively low NaOCl doses (1–3 mg/L) and moderate DO concentrations (4–5 mg/L). This enhanced performance is attributed to the rapid initial oxidation of $Fe^{2+}$ by NaOCl, generating reactive ferric species that, upon aeration, improve floc formation, aggregation, and settling. In contrast, applying chlorination after aeration does not fully exploit this synergistic effect, highlighting the treatment sequence as a critical design and operational parameter. These findings extend existing research by providing experimental evidence that underscores the importance of treatment sequence in optimizing combined iron removal systems.

A further innovation of this study is the development of a Gene Expression Programming (GEP) model to predict the optimal NaOCl dose required for effective iron removal. The GEP model exhibited strong predictive performance, with a coefficient of determination ($R^2$) of approximately 0.94 and a root mean square error (RMSE) of approximately 0.34 mg/L. These results are comparable to, and in some cases exceed, the predictive accuracy of other machine learning techniques such as Artificial Neural Networks (ANNs) and Support Vector Machines (SVMs), which are commonly applied in water treatment modeling. However, unlike ANN and SVM approaches, which typically function as “black-box” models, GEP generates explicit mathematical expressions that directly relate input parameters—such as pH, DO, and influent iron concentration—to the required NaOCl dose. This interpretability represents a significant advantage, particularly when working with relatively small datasets, as in the present study. Sensitivity analysis further revealed that pH and DO exert comparable influences on oxidant demand, with their effects slightly exceeding that of the initial iron concentration, in agreement with the chemical kinetics governing iron oxidation. Collectively, these results demonstrate that GEP is well-suited for decision-support applications and could be effectively integrated into automated dosing and control systems for groundwater treatment facilities.

Many studies on iron removal emphasize treatment performance; explicit cost analysis is often neglected despite its importance for practical implementation. In this study, a comparative cost assessment indicated that aeration alone represents the most energy-intensive option, whereas chemical oxidation incurs higher chemical costs. The combined pre-chlorination–aeration strategy achieved an approximate 42.7% reduction in overall treatment cost relative to aeration alone, without compromising removal efficiency. This reduction is primarily attributable to decreased aeration energy requirements, enabled by the initial chemical oxidation step. By explicitly linking treatment performance to operational costs, this study provides a practical framework for selecting and optimizing iron-removal strategies in real-world applications. The integration of experimental investigation, predictive modeling, and economic evaluation constitutes a meaningful contribution to the literature. It enhances the practical relevance of the findings for engineers, operators, and decision-makers in the water treatment sector.

## 6. LIMITATIONS

Despite the insights this study provides, several limitations should be considered when interpreting the results. The experimental investigation was conducted under controlled laboratory-scale conditions, which allowed systematic evaluation of key parameters but did not fully capture the hydraulic complexity, influent variability, and long-term operational dynamics characteristic of pilot- or full-scale groundwater treatment systems. Factors such as fluctuating flow regimes, aging of treatment media, and seasonal variations in water quality may influence iron removal performance under real-world conditions; therefore, direct extrapolation of the findings to full-scale applications should be approached with caution.

In addition, disinfection by-products (DBPs), particularly trihalomethanes (THMs), were not analyzed despite the use of sodium hypochlorite as an oxidant. While the study focused on iron removal efficiency and oxidation behavior, the absence of DBP monitoring limits the ability to assess potential public health implications associated with chlorination under the investigated conditions. Furthermore, the gene expression programming (GEP) model was developed using a relatively small dataset (n = 56). Although appropriate

validation techniques were applied, the limited dataset may restrict model robustness and generalizability. Accordingly, the proposed model should be regarded primarily as an interpretative tool for exploring relationships between operational parameters and iron removal efficiency, rather than as a fully generalized predictive model. Expanded datasets and validation under pilot- and full-scale conditions are recommended in future research.

## 7. CONCLUSION

This study investigated the removal of iron from groundwater using sodium hypochlorite oxidation, aeration, and their combined application, with particular emphasis on oxidation mechanisms, operational feasibility, and predictive modeling.

First, the results confirm that iron oxidation efficiency is strongly influenced by pH-dependent oxidant speciation and dissolved oxygen availability. Although highly acidic conditions (pH = 4) promote rapid iron oxidation due to the predominance of hypochlorous acid, this outcome should be interpreted primarily as a fundamental kinetic insight rather than a practical operational target. Under near-neutral conditions (pH 6.5–7.5), which are more representative of real-world groundwater treatment systems, effective iron removal was achieved through appropriate oxidant dosing and dissolved oxygen control.

Second, from an operational standpoint, the combined pre-chlorination-aeration treatment strategy emerged as the most balanced and practical approach. The application of a low-sodium hypochlorite dose (1–3 mg $L^{-1}$) before aeration, coupled with an increase in dissolved oxygen to approximately 4–5 mg $L^{-1}$, consistently achieved iron removal efficiencies ranging from 85% to 89%. This integrated strategy provides a favorable compromise between treatment efficiency, chemical consumption, and energy demand, rendering it more suitable for practical groundwater treatment applications than either aeration or chemical oxidation applied independently.

Third, gene expression programming (GEP) proved to be a robust, interpretable predictive tool for estimating the required oxidant dose across varying operational conditions. Unlike black-box machine learning approaches, the GEP framework produces explicit mathematical expressions that directly relate operational variables to treatment performance. These equations can be readily implemented for decision support and process optimization without reliance on complex programming environments, facilitating potential integration into automated or semi-automated control systems.

The findings demonstrate that integrating controlled oxidation–aeration strategies with interpretable, data-driven modeling enhances both mechanistic understanding and operational decision-making in groundwater iron removal processes.

Future research should focus on validating the proposed treatment strategy at pilot and full scales, incorporating disinfection by-product (DBP) analyses—particularly trihalomethanes—to evaluate potential public health implications, and expanding the modeling framework using larger datasets that incorporate real-time sensor inputs (e.g., pH, dissolved oxygen, total organic carbon, and manganese). These efforts will further improve model robustness, generalizability, and practical applicability.

### ACKNOWLEDGMENTS

The authors would like to express their deepest gratitude to the University, participants and colleagues for their exceptional support and resources, which were critical in facilitating this research.

### CONFLICTS OF INTEREST

The authors declare that no conflicts of interest are associated with this study. All aspects of the research were conducted with the utmost integrity and transparency.

### DATA AVAILABILITY

The datasets utilized and analyzed during this research are available from the corresponding author upon reasonable request.

### ETHICAL STATEMENTS

The authors confirm that the study complied with all applicable local laws, ethical standards, and institutional guidelines, including obtaining approval from relevant ethics committees.

### FUNDING

This research was conducted without financial support. The authors confirm that no funding was received for this study's research, analysis, or publication.

## REFERENCES

[1] T. L. Jolaosho, A. A. Mustapha, and S. T. Hundeyin, “Hydrogeochemical evolution and heavy metal characterization of groundwater from southwestern, Nigeria: An integrated assessment using spatial, indexical, irrigation, chemometric, and health risk models,” Heliyon, vol. 10, no. 19, 2024, https://doi.org/10.1016/j.heliyon.2024.e38364

[2] A. J. Natishah, M. S. Samuel, K. Velmurugan, S. R. Showparnickaa, S. M. Indumathi, and M. Kumar, “Contamination of groundwater by microorganisms and risk management: Conceptual model, existing data, and challenges,” Groundw. Sustain. Dev., vol. 29, p. 101408, 2025, https://doi.org/10.1016/j.gsd.2025.101408

[3] R. D. Alsaeed, B. Alaji, and L. Khouri, “Modeling chlorine residuals in urban water distribution networks (Al-Ashrafieh - Homs),” Environ. Res. Commun., vol. 6, no. 8, p. 81001, 2024, https://doi.org/10.1088/2515-7620/ad64b3

[4] World Health Organization (WHO), The World Health Report 2000 - Health Systems: Improving Performance. Geneva, Switzerland: World Health Organization, 2000.

[5] A. G. Tekerlekopoulou and D. V. Vayenas, “Simultaneous biological removal of ammonia, iron and manganese from

potable water using a trickling filter," Biochem. Eng. J., vol. 39, no. 1, pp. 215–220, 2008, https://doi.org/10.1016/j.bej.2007.09.005

[6] K. Teunissen, A. Abrahamse, H. Leijssen, L. Rietveld, and H. van Dijk, "Removal of both dissolved and particulate iron from groundwater," Drink. Water Eng. Sci. Discuss., vol. 1, no. 1, pp. 87–115, 2008, https://doi.org/10.5194/dwesd-1-87-2008

[7] H. A. Aziz, H. A. Tajarudin, T. H. L. Wei, and M. Y. D. Alazaiza, "Iron and manganese removal from groundwater using limestone filter with iron-oxidized bacteria," Int. J. Environ. Sci. Technol., vol. 17, no. 5, pp. 2667–2680, 2020, https://doi.org/10.1007/s13762-020-02681-5

[8] M. Deborde and U. von Gunten, "Reactions of chlorine with inorganic and organic compounds during water treatment-Kinetics and mechanisms: A critical review," Water Res., vol. 42, no. 1–2, pp. 13–51, 2008, https://doi.org/10.1016/j.watres.2007.07.025

[9] Tech Brief, "Iron and Manganese Removal," A national Drinking water Clearinghouse Sheet, 1998. https://actat.wvu.edu/files/d/a0d141dd-f559-412b-91df-bd1d14c52545/iron-mn-removal.pdf

[10] D. A. Lytle, D. Williams, C. Muhlen, E. Riddick, and M. Pham, "The removal of ammonia, arsenic, iron and manganese by biological treatment from a small Iowa drinking water system," Environ. Sci. Water Res. Technol., vol. 6, no. 11, pp. 3142–3156, 2020, https://doi.org/10.1039/d0ew00361a

[11] C. Lytle and M. Edwards, "Mechanistic Study of Iron Sequestration by Phosphates," ACS ES&T Water, vol. 5, no. 9, pp. 5309–5317, 2025, https://doi.org/10.1021/acsestwater.5c00411

[12] World Health Organization, A global overview of national regulations and standards for drinking-water quality. World Health Organization, 2021. [Online]. Available: https://www.who.int/publications/i/item/9789241513760

[13] F. Kozisek, "Regulations for calcium, magnesium or hardness in drinking water in the European Union member states," Regul. Toxicol. Pharmacol., vol. 112, p. 104589, 2020, https://doi.org/10.1016/j.yrtph.2020.104589

[14] L. L. Pin, "Removal of Iron From Water Using Oxidation Process," Universiti Tunku Abdul Rahman, 2021. [Online]. Available: http://eprints.utar.edu.my/5372/2/1603590_FYP.pdf

[15] G. Tredoux, S. Clarke, and L. C. Cavé, "The feasibility of in situ groundwater remediation as robust low-cost water treatment option," Gezina, South Africa, 2004. [Online]. Available:https://www.wrc.org.za/wp-content/uploads/mdocs/1325-1-041.pdf

[16] M. Ghosh, "A study of the rate of oxidation of iron in aerated ground waters," Dept. of Civil Engineering, University of Illinois, Urbana, 1962. [Online]. Available: https://www.ideals.illinois.edu/items/45718/bitstreams/135347/data.pdf

[17] J. F. Mcpeak and H. L. Aronovitch, "Iron in water and processes for its removal," 21st Annu. Lib. Bell Corros. Course, 1983.

[18] J. Vercellotti, "Kinetics of Iron Removal Using Potassium Permanganate and," Challenge. Ohio University, 1988.

[19] C. C. Kan, M. W. Wan, W. H. Chen, P. Phatai, J. Wittayakun, and K. F. Li, "The preliminary study of iron and manganese removal from groundwater by NaOCl oxidation and MF filtration," Sustain. Environ. Res., vol. 22, no. 1, pp. 25–30, 2012. https://hero.epa.gov/reference/8222139/

[20] F. Mamadou, S. F. Mbacké, D. E. H. Moussa, T. A. Ousmane, M. F. Aminata, and D. M. C. Guèye, "Iron in Water: Study of Iron Removal Kinetics in Chemically Reconstituted Waters: Application to Groundwater of South Pout (PS2 Site)," Open J. Met., vol. 11, no. 01, pp. 1–10, 2021, https://doi.org/10.4236/ojmetal.2021.111001

[21] R. Buamah, B. Petrusevski, and J. C. Schippers, "Oxidation of adsorbed ferrous iron: Kinetics and influence of process conditions," Water Sci. Technol., vol. 60, no. 9, pp. 2353–2363, 2009, https://doi.org/10.2166/wst.2009.597

[22] D. Vries et al., "Iron and manganese removal: Recent advances in modelling treatment efficiency by rapid sand filtration," Water Res., vol. 109, pp. 35–45, 2017, https://doi.org/10.1016/j.watres.2016.11.032

[23] H. Kang, Y. Liu, D. Li, and L. Xu, "Study on the Removal of Iron and Manganese from Groundwater Using Modified Manganese Sand Based on Response Surface Methodology," Appl. Sci., vol. 12, no. 22, p. 11798, 2022, https://doi.org/10.3390/app122211798

[24] D. Propolsky and V. Romanovski, "Iron and manganese removal from groundwater: comprehensive review of filter media performance and pathways to polyfunctional applications," Environ. Sci. Water Res. Technol., 2025, https://doi.org/10.1039/d5ew00751h

[25] M. F. Naamah, "Smart Management of Fresh Water Uses in Syria Using a Neural Network Model," Steps Civil, Constr. Environ. Eng., vol. 1, no. 2, pp. 40–50, 2023, https://doi.org/10.61706/sccee12011165

[26] R. Alsaeed, "Modelling turbidity removal by poly-aluminium chloride coagulant using gene expression," Adv. Environ. Technol., vol. 7, no. 4, pp. 263–273, 2021, https://doi.org/10.22104/AET.2022.5303.1433

[27] G. Volf, M. Krbavčić, I. Sušanj Čule, and S. Zorko, "Prediction Models for Manganese, Iron and Ammonium in Raw Water for a Drinking Water Treatment Plant Butoniga (Croatia)," Eng. Rev., vol. 43, no. 3, pp. 68–80, 2023, https://doi.org/10.30765/er.2232

[28] R. D. Alsaeed, B. Alaji, and M. Ibrahim, "Modeling Jar Test Results Using Gene Expression to Determine the Optimal Alum Dose in Drinking Water Treatment Plants," Baghdad Sci. J., vol. 19, no. 5, pp. 951–965, 2022, https://doi.org/10.21123/bsj.2022.6452

[29] S. McKelvey, A. Abassi, C. Nataraj, and M. Duran, "Data-driven modeling techniques for prediction of settled water turbidity in drinking water treatment," Front. Environ. Eng., vol. 3, p. 1401180, 2024.

[30] A. M. Shrestha, S. Kazama, B. Sawangjang, and S. Takizawa, "Improvement of Removal Rates for Iron and Manganese in Groundwater Using Dual-Media Filters Filled with Manganese-Oxide-Coated Sand and Ceramic in Nepal," Water (Switzerland), vol. 16, no. 17, p. 2450, 2024, https://doi.org/10.3390/w16172450

[31] H. Daraei et al., "DOC signal-based alum dose control for drinking water treatment plants," J. Water Process Eng., vol. 54, p. 103934, 2023, https://doi.org/10.1016/j.jwpe.2023.103934

[32] H. Shin et al., "Development of water quality prediction model for water treatment plant using artificial intelligence algorithms," Environ. Eng. Res., vol. 29, no. 2, 2024, https://doi.org/10.4491/eer.2023.198

[33] R. D. Alsaeed, B. Alaji, and M. Ibrahim, "Predicting aluminium using full-scale data of a conventional water

treatment plant on Orontes River by ANN, GEP, and DT," Int. J. Water, vol. 15, no. 3, pp. 190–206, 2023, https://doi.org/10.1504/IJW.2023.133991

[34] M. E. Sutharsan, S. P. S. Meegahakumbura, and N. S. Miguntanna, "Removal of Manganese and Iron from Groundwater by using Chlorination and Rapid Sand Filtration: A Case Study," Eng. J. Inst. Eng. Sri Lanka, vol. 56, no. 2, pp. 13–21, 2023, https://doi.org/10.4038/engineer.v56i2.7529

[35] C. Ferreira, "Genetic Representation and Genetic Neutrality in Gene Expression Programming," Adv. Complex Syst., vol. 05, no. 04, pp. 389–408, 2002, https://doi.org/10.1142/s0219525902000626

[36] C. Ferreira, "Function Finding and the Creation of Numerical Constants in Gene Expression Programming," in Advances in Soft Computing, Springer, 2003, pp. 257–265. https://doi.org/10.1007/978-1-4471-3744-3_25

[37] C. Ferreira, "Gene Expression Programming in Problem Solving," in Soft Computing and Industry, Springer, 2002, pp. 635–653. https://doi.org/10.1007/978-1-4471-0123-9_54

[38] N. Lewis-Rogers, K. A. Crandall, and D. Posada, Evolutionary analyses of genetic recombination. Kerala, India: Research Signpost, 2004. [Online]. Available: https://www.academia.edu/download/71599964/Evolutionary_analyses_of_genetic_recombi20211006-16515-6o5zej.pdf

[39] M. Achite et al., "Modern Techniques to Modeling Reference Evapotranspiration in a Semi-arid Area Based on ANN and GEP Models," Water (Switzerland), vol. 14, no. 8, p. 1210, 2022, https://doi.org/10.3390/w14081210

[40] Hach Company, DR 2010 Spectrophotometer Instrument Manual. Loveland, USA: Hach Company, 1999. [Online]. Available: http://www.fieldenvironmental.com/assets/files/Manuals/HACH Spectrophotometer DR2010 Manual.pdf

[41] C. Ferreira, "Gene Expression Programming: a New Adaptive Algorithm for Solving Problems," arXiv Prepr. cs/0102027, 2001, [Online]. Available: http://arxiv.org/abs/cs/0102027

[42] T. Thinojah and B. Ketheesan, "Iron removal from groundwater using granular activated carbon filters by oxidation coupled with the adsorption process," J. Water Clim. Chang., vol. 13, no. 5, pp. 1985–1994, 2022, https://doi.org/10.2166/wcc.2022.126

[43] B. & V. Corporation, White's Handbook of Chlorination and Alternative Disinfectants: Fifth Edition. John Wiley & Sons, 2010. https://doi.org/10.1002/9780470561331

[44] T. X. Wang and D. W. Margerum, "Kinetics of Reversible Chlorine Hydrolysis: Temperature Dependence and General-Acid/Base-Assisted Mechanisms," Inorg. Chem., vol. 33, no. 6, pp. 1050–1055, 1994, https://doi.org/10.1021/ic00084a014

[45] D. Li, Y. Zhuang, Y. Hua, and B. Shi, "Effect of free chlorine on drinking water quality in old unlined cast iron pipes," Chinese J. Environ. Eng., vol. 17, no. 2, pp. 675–681, 2023, https://doi.org/10.12030/j.cjee.202209001